

Short Communication

Electrochemical Biosensor for the Determination of Sufentanil in Human Plasma and Urine based on TiO₂-Graphene Composite modified carbon paste electrode

Hongchao Zhang*, Youli He

Department of Clinical Medicine, Heze Medical College, Heze, 274000, China

*E-mail: furuiteng345678@126.com

Received: 2 May 2021/ Accepted: 29 June 2021 / Published: 10 August 2021

In this work, the synthesis of TiO₂ and graphene nanocomposite modified carbon paste electrode (TiO₂-GO/CPE) as an electrochemical biosensor for the detection of sufentanil in human plasma and urine was investigated. The modified Hummers approach was used to synthesize GO nanosheets, and the hydrothermal approach was used to produce TiO₂-GO nanocomposite. Due to the interaction of TiO₂ nanoparticles with GO, structural studies of the produced nanocomposite using SEM and XRD revealed that TiO₂ nanoparticles in anatase structure had been anchored to GO's nanosheets surface. Electrochemical studies using CV revealed that TiO₂-GO/CPE had higher electrocatalytic current and lower potential than GO/CPE and CPE for determination of sufentanil due to the synergetic effect of high electrical conductivity of GO nanosheets and intercalation of TiO₂ nanoparticles on nanocomposites. The sensitive, stable, and rapid response of TiO₂-GO/CPE was demonstrated in amperometric tests for the detection of sufentanil. The limit of detection, sensitivity and linear range for the determination of sufentanil was obtained at 0.07nM, 4.1070μA/μM, and 1 to 10 μM, respectively. The ability of TiO₂-GO/CPE as a sufentanil sensor in prepared real samples of urine and human plasma showed that the performance of TiO₂-GO/CPE to determine sufentanil in real samples was adequate and acceptable.

Keywords: Sufentanil detection; Hydrothermal technique; TiO₂ Nanoparticles; Graphene oxide; Amperometry

1. INTRODUCTION

Sufentanil(N-[4-(methoxymethyl)-1-(2-thiophen-2-ylethyl)piperidin-4-yl]-N-phenylpropanamide) as a synthetic opioid analgesic drug is a derivative of fentanyl [1, 2]. It can be synthesized by the addition of a methoxymethyl group on the piperidine ring of fentanyl which makes it more rapid onset, more potent analgesic and short duration of action than fentanyl [3-5]. This opioid use as medicine for pain relief, induction and maintenance of anaesthesia in surgery and post-operative

pain management because it has potency to form the strong binding affinity and rapid displacement of buprenorphine from the opioid receptors in the central nervous system and control postoperative pain, induction of anaesthesia, and provide analgesia [6-8].

Management of the drug doses is essential because sufentanil like as potent and sophisticated prescription medicine come with side effects such as significant respiratory depression, respiratory arrest, heart rhythm irregularity, muscle stiffness/rigidity, blood pressure changes drowsiness, itching and nausea/vomiting [9, 10]. Therefore, practitioners must follow patients for signs and symptoms of respiratory depression and sedation [11, 12]. Therefore, determination the sufentanil dosage and level in human urine and blood is very important, and many studies have been performed to develop the sensitive and fast technique of determination of sufentanil.

High performance liquid chromatography [13], gas chromatography [14], mass spectrometry [15], flame ionization [16] and Ultra-performance liquid-chromatography [17, 18] are the most widely used techniques for detection sufentanil in samples. The electrochemical techniques are low cost and fast analytical tool for determination of trace concentrations of various species in human urine and blood samples [19-21]. Modification of the electrode surface by various nanostructures and compositions in electrochemical methods can enhance the sensitivity and accuracy [22-24]. Nonetheless, not much study has been carried out so far to identify the sufentanil by electrochemical methods [25-27]. Therefore, this study was conducted on the synthesis of TiO₂-Graphene composite as electrochemical biosensor for the determination of sufentanil in human plasma and urine.

2. MATERIALS AND METHOD

In order to prepare the carbon paste electrode, the homogeneous paste of prepared graphite powder and paraffin oil in a weight ratio of 7:3 was provided less than 30°C and transferred to a hollow polytetrafluoroethylene tube (PTFE, Sigma-Aldrich) which contained electrical contact by a copper wire. After cooling, the surface of the paste was smoothed with soft paper. Then, the prepared CPE was rinsed with DI water.

The modified Hummers method was employed for the preparation of GO as following procedure [28]: the homogeneous mixture of 1 g graphite powder (99%, Topfly Material Co., Ltd., China), 25 mL H₂SO₄ (99%, Hebei Dongding Chemical Trade Co., Ltd., China) and 100 g NaNO₃ (≥99.0%, Sigma-Aldrich) was prepared in 250 mL volumetric flask under magnetic stirring in ice-bath for 30 minutes. Next, 3 g KMnO₄ (97%, Sigma-Aldrich) and 190 mL deionized (DI) water was slowly added to the mixture under magnetic stirring at 40°C for 30 minutes. Afterward, 10 mL H₂O₂ (30%, Shijiazhuang Chemical Tech Co., Ltd., China) was added to the obtained suspension. The unexfoliated graphite particles in the resulted mixture were removed through centrifugation at 1000 rpm for 5 minutes and filtration, respectively. The final mixture was washed, and then transferred to the oven and dried at 70 °C for 12 hours.

TiO₂-GO nanocomposite was prepared through the hydrothermal method. In order to the synthesis of TiO₂-GO composite in a molar ratio of 7:10 of TiO₂ and GO, the homogeneous mixture of 20 mg of the obtained graphene powder, 5 mL of 1 M H₂SO₄ (99.999%, Sigma-Aldrich) and 0.1 mL of

titanium isopropoxide (97%, Sigma-Aldrich) was ultrasonically prepared for 15 minutes. Subsequently, the mixture was transferred to a 25 mL Teflon-lined stainless-steel autoclave. It was sealed and heated at 180 °C for 24 hours in the oven. 10 mg of the obtained TiO₂-GO nanocomposite was ultrasonically dispersed in 10 mL of dimethylformamide (DMF, 99.8%, Merck) for 1 hour to reach a homogenous suspension. Next, 10 μL of the final product was slowly dropped onto the surface of prepared CPE and dried at room temperature.

The sufentanil-negative serum and urine samples of middle-aged men were provided from Beijing Hospital (Beijing, China). 1 mL of samples was diluted to 10 mL with the buffer solution (pH 7). The standard addition method was applied through spike the specified amounts of sufentanil in the prepared real samples. The spiked samples were stored in the refrigerator at 4 C°.

Cyclic voltammetry (CV) and amperometry techniques were applied for electrochemical studies of prepared electrodes using potentiostatAutolab PG- STAT302N (Metrohm, EcoChimie B.V., Utrecht, The Netherlands) in standard three-electrode cell. The electrochemical cell was contained the prepared electrode (CPE, GO/CPE or TiO₂-GO/CPE) as working electrode, platinum wire as a counter electrode, and Ag/AgCl (3M KCl) as reference electrode. 0.1 M NaCl solution (≥ 99.5%, Merck) (pH 7) was used as supporting electrolyte. Characterization of the morphology and crystal structure of the synthesized GO and nanocomposite were carried out using scanning electron microscopy (SEM, Hitachi S-3000N, Japan) and X-ray diffractometer (XRD, Cu Kα₁ radiation (λ = 1.5406 nm), operating voltage of 40 kV and current of 35 mA, Thermo scientific, ARL X'TRA).

3. RESULT AND DISCUSSION

3.1 Characterization the morphology and crystal structure of the synthesized GO and TiO₂-GO nanocomposite

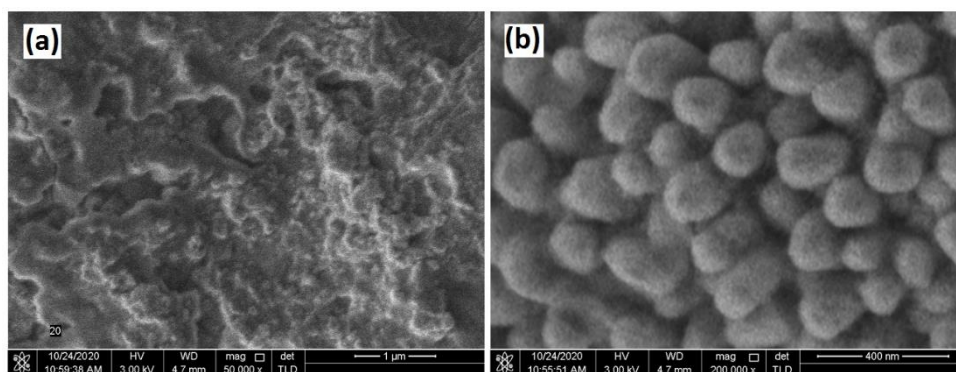


Figure 1. SEM images of (a) GO/CPE and (b) TiO₂-GO/CPE.

Figure 1a depicts SEM images of GO/CPE that exhibit the thin layer of graphene oxide with irregular and coarse structures covered the surface of the CPE because of the planar configuration of graphene nanosheets on graphite structure [29]. Furthermore, the functional groups on GO tend to gather in clusters rather than be evenly distributed [30]. Figure 1b shows the morphology of TiO₂-GO

nanocomposite on CPE. As seen, TiO₂ nanoparticles have been anchored on GO's nanosheets surface due to the interaction of TiO₂ nanoparticles with GO during the hydrothermal procedure [31, 32].

The crystal structure analysis of powder of GO and TiO₂-GO nanocomposite is shown in the XRD patterns of Figure 2. As seen from Figure 2a, the XRD pattern of GO shows the characteristic diffraction peak at 10.43° and 42.15°, corresponding the successful oxidation of graphite into GO with (002) and (100) planes, respectively [33-35]. XRD pattern of TiO₂-GO nanocomposite in Figure 2b displays the characteristic peaks at 25.02°, 37.15°, 47.81°, 54.89° and 62.09° which indicated to the anatase structure of TiO₂ with (101), (004), (200), (211) and (204) planes (JCPDS Card no. 21-1272), respectively. Moreover, the disappearance of (002) and (100) peaks of GO reveal that the intercalation of TiO₂ nanoparticles could destroy the crystal orientation and regular stack of GO nanosheets [36]. The results are in agreements with the SEM analyses of synthesized GO nanosheets and TiO₂-GO nanocomposite on CPE.

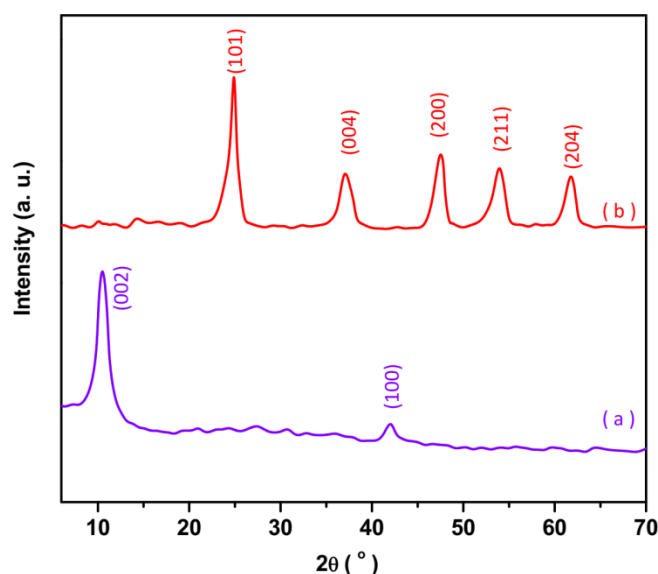


Figure 2. XRD patterns of powder of (a) GO and (b) TiO₂-GO.

3.2 Electrochemical characterization of prepared electrodes

The CV curves of CPE, GO/CPE and TiO₂-GO/CPE in 0.1 M NaCl (pH 7) solution at 15mV/s in the potential range of -0.10 to 0.75 V are shown in Figure 3. Before addition the sufentanil (Figure 3a), it isn't observed any redox peak for all electrodes. After addition of the 5μM sufentanil (Figure 3b), the broad shoulder as an anodic peak appears at 0.50 V for CPE. The CV curves of GO/CPE and TiO₂-GO/CPE show the irreversible oxidation peaks at 0.60 V and 0.33 V with the current of 14.05 μA and 18.89 μA, respectively. The high electrocatalytic current and lower potential obtained for TiO₂-GO/CPE that it can be attributed to the synergetic effect of high electrical conductivity of GO nanosheets and intercalation of TiO₂ nanoparticles on nanocomposites, and resulted in high porosity and an absorbent layer of heterostructure of TiO₂-GO on CPE. Moreover, inbuilt oxygen vacancies as

electron production states have been created through the Ti^{4+} , Ti^{3+} and O^{2-} interstitials of TiO_2 NPs that facilitated the density of active sites [37-39]. It is suggested that TiO_2 shows a negative zeta potential and preparation nanocomposite of TiO_2 with the negatively charged GO can be formed more negatively charged nanocomposite of TiO_2 -GO which associated with the electrostatic interaction of TiO_2 -GO with the positively charged sufentanil ions in the solution [40, 41]. In addition, GO contain certain amounts of oxygen functional groups, such as hydroxyl, epoxide, and carbonyl groups which have a significant effect on the electronic properties, work function and band gap [42]. The Ti-O-C and Ti-C interfacial bonds and strong electronic hybridization of TiO_2 with GO have been formed in TiO_2 -GO nanocomposites due to anchoring of carbon flakes or polyaromatic hydrocarbons of GO on TiO_2 by bridging oxygen atom of functional groups in the hydrothermal process [30]. The studies in TiO_2 -GO nanocomposites have been shown that charge depletion and charge accumulation are happening at the interface of GO and TiO_2 which indicated to interfacial cross-links and effective pathway for fast charge transfer from RGO to TiO_2 in electrochemical reactions [30, 43].

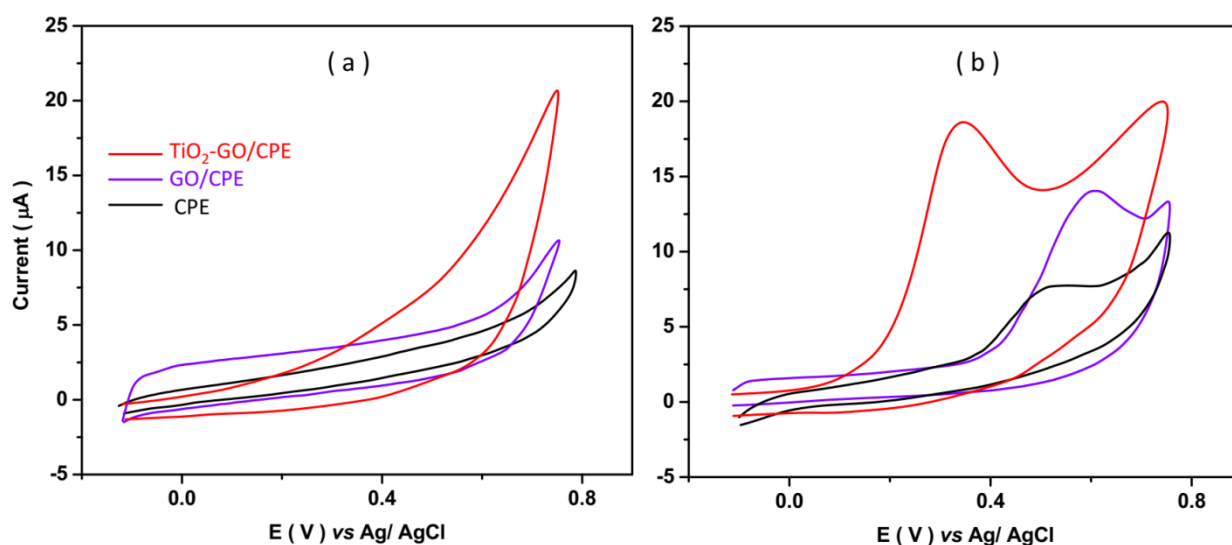


Figure 3. The CV curves of CPE, GO/CPE and TiO_2 -GO/CPE in 0.1 M NaCl (pH 7) solution at 15 mV/s in the potential range of -0.10 to 0.75 V (a) before and (b) after addition of 5 μM sufentanil.

Further electrochemical studies were conducted on amperometry technique in 0.1 M NaCl (pH 7) with speed rotation of 1000 rpm at a potential of 0.50, 0.60 and 0.33 V for CPE, GO/CPE and TiO_2 -GO/CPE, respectively. Figure 4 reveals the creation of electrocatalytic current after the addition of 10 μM sufentanil at the second minute. The highest and fastest response is obtained for TiO_2 -GO/CPE. The investigation of the stability of signal from second to 10th minute displays that change of 28, 17 and 3% of amperometric signals of CPE, GO/CPE and TiO_2 -GO/CPE, respectively, indicating low stability of response of CPE and GO/CPE for the determination of sufentanil, and more stable the response is observed for TiO_2 -GO/CPE due to fast charge transfer and the formed cross-links and strong binding in the composite, such as Ti-O-C and Ti-O-H...O-C bonds, between GO and TiO_2

[30, 44], which provide a more and stable electroactive site on the composite surface. Therefore, the TiO₂-GO/CPE was selected as the fast, sensitive and stable sufentanil sensor among the prepared electrodes for the following studies.

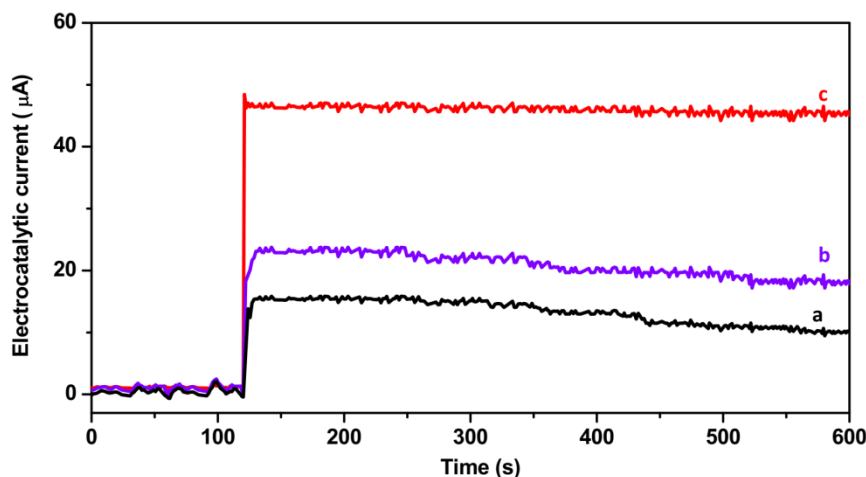
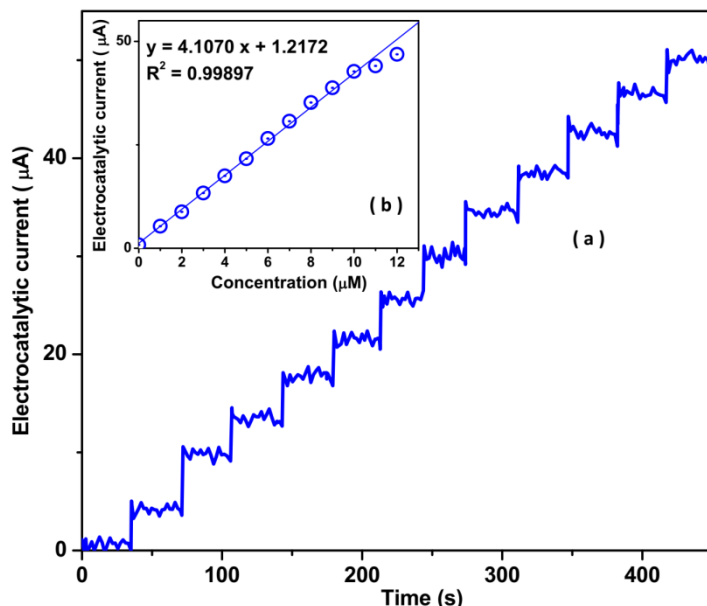


Figure 4. The amperometry response in 0.1 M NaCl (pH 7) with speed rotation of 1000 rpm before and after addition of 10 μM sufentanil for (a) CPE, (b) GO/CPE and (c) TiO₂-GO/CPE at potential of 0.50, 0.60 and 0.33 V, respectively.

To evaluate the sensitivity, linear range, and detection limit values of TiO₂-GO/CPE as sufentanil sensor, the amperometry response in 0.1 M NaCl (pH 7) with speed rotation of 1000 rpm at the potential of 0.33 V under successive addition of 1 μM sufentanil was studied. Figures 5a and 5b exhibit the recorded amperograms and obtained calibration plot of TiO₂-GO/CPE, signifying to linearly increasing the electrocatalytic current with increasing the sufentanil concentration. The limit of detection and sensitivity is obtained at 0.07nM and 4.1070 $\mu\text{A}/\mu\text{M}$, respectively. Furthermore, the resulted calibration plot that it demonstrates 1 to 10 μM as the linear range for determination of sufentanil on TiO₂-GO/CPE.

In addition, the performance of TiO₂-GO/CPE for determination of sufentanil is compared with other sensors in the literature in Table 1. As observed, the TiO₂-GO/CPE performance is comparable or better than other reported sufentanil sensors. Besides, the wide linear range of TiO₂-GO/CPE can be related to interactions of N-H coordination bond on TiO₂ and π conjugation of GO with aromatic rings of sufentanil that it facilitates the adsorption of sufentanil on the composite surface [40]. Therefore, the synergetic effect of GO and TiO₂ can extend the density of effective active sites, effective surface area and electrical conductivity which can enhance the interfacial contact between the electrolyte and electrode and improve the accessibility of sufentanil [45-49].



Figures 5. The amperometric response and obtained calibration plot of $\text{TiO}_2\text{-GO/CPE}$ in 0.1 M NaCl (pH 7) with speed rotation of 1000 rpm at potential of 0.33 V under successive addition of 1 μM sufentanil.

Table 1. Comparison of performance of $\text{TiO}_2\text{-GO/CPE}$ with other sufentanil sensors in the literature.

Technique	Detection limit (nM)	Linear range (μM)	Ref.
(HF-LLLME) ^a - (HPLC-DAD) ^b	5.9	0.012-2.59	[13]
DLLME ^c -HPLC-DAD	4.9	0.012-2.59	[13]
SPE-GC-MS ^d	0.0064	2.5×10^{-6} - 5.17×10^{-5}	[14]
SPE-GC-MS	0.129	0.0012-0.012	[15]
SDME-GC-FID ^e	12.1	0.029-2.59	[16]
UPLC-MS/MS ^f	0.183	1.83×10^{-4} -0.0117	[17]
LC-MS/MS ^g	0.776	7.76×10^{-4} -0.005	[50]
DPV ^h with MWCNTs/SPCE ⁱ	20	0.064 - 3.62	[25]
AMP ^j with $\text{TiO}_2\text{-GO/CPE}$	0.07	1-10	This work

^aHollow fiber liquid-liquid-liquid microextraction; ^bhigh performance liquid chromatography with diode-array detector; ^cDispersive liquid-liquid microextraction; ^dSolid phase extraction-gas chromatography-mass spectrometry; ^eSingle drop microextraction-gas chromatography-flame ionization detection; ^fUltra-performance liquid-chromatography mass-spectrometry; ^gLiquid chromatography-tandem mass spectrometry; ^hDifferential pulse voltammetry; ⁱScreen-printed carbon electrode; ^jAmperometry

The interference effect of proposed sufentanil sensor was studied in presence of biological species in human serum and urine samples which presented in Table 2. Table 2 shows the amperometric current of $\text{TiO}_2\text{-GO/CPE}$ in 0.1 M NaCl (pH 7) with a speed rotation of 1000 rpm at the

potential of 0.33 V under successive addition of 0.5 μM sufentanil and 2 μM of interfering substrates. It can be observed that a significant signal is obtained for injection of sufentanil, and there is a negligible signal to injection of interfering substrates at 0.33 V, indicating to the substrates in Table 2 doesn't exhibit interference with the detection of sufentanil by $\text{TiO}_2\text{-GO/CPE}$. Thus, it is demonstrated to great selectivity of prepared sufentanil sensor.

Table 2. Amperometric current of $\text{TiO}_2\text{-GO/CPE}$ in 0.1 M NaCl (pH 7) with speed rotation of 1000 rpm at potential of 0.33 V under successive addition of 0.5 μM sufentanil and 2 μM of interfering substrates

Substance	Added (μM)	amperometric current signal (μA)	RSD (%)
sufentanil	0.5	2.041	± 0.071
K^+	2	0.100	± 0.004
Mg^{2+}	2	0.091	± 0.007
Ca^{2+}	2	0.093	± 0.003
CO_3^{2-}	2	0.074	± 0.004
HCO_3^-	2	0.110	± 0.010
PO_4^{3-}	2	0.109	± 0.050
SO_4^{2-}	2	0.097	± 0.008
Glucose	2	0.109	± 0.009
ammonia	2	0.087	± 0.004
creatinine	2	0.057	± 0.006
Uric acid	2	0.099	± 0.007
Urea	2	0.101	± 0.009

The $\text{TiO}_2\text{-GO/CPE}$ ability was investigated for the analysis of sufentanil in prepared real samples of urine and human plasma through the standard addition method. Amperometry measurements were carried out on the modified electrode in 0.1 M NaCl (pH 7) prepared of real samples with speed rotation of 1000 rpm at the potential of 0.33 V. Table 3 presents the sufentanil concentration of real samples and recovery and relative standard deviation (RSD) of spiked levels in urine and human plasma. The observation are indicated that there are no sufentanil in both samples, and the recovery and RSD values are in the range of 94.0 to 98.7% and 2.85 to 4.07%, respectively, illustrating satisfactory and acceptable precision of performance of $\text{TiO}_2\text{-GO/CPE}$ to determination of sufentanil in real samples.

Table 3. Analytical results of determination of sufentanil levels in prepared real samples of urine and human plasma on $\text{TiO}_2\text{-GO/CPE}$.

Sample	Added (μM)	Found (μM)	Recovery (%)	RSD (%)
urine	0.00	0.00	Not detected	-
	1.00	0.94	94.0	4.07
	2.00	1.91	95.5	3.51
	5.00	4.85	97.0	2.85

	10.00	9.77	97.7	3.25
plasma	0.00	0.00	Not detected	-
	1.00	0.96	96.0	3.31
	2.00	1.93	96.5	2.81
	5.00	4.79	95.8	3.05
	10.00	9.87	98.7	3.58

4. CONCLUSION

In this work, the synthesis of TiO₂-GO/CPE as an electrochemical biosensor for the detection of sufentanil in human plasma and urine were described. GO nanosheets was synthesized by the modified Hummers method and hydrothermal method were used for the synthesis of GO and TiO₂-GO nanocomposite, respectively. The structural analyses of prepared nanocomposite demonstrated that TiO₂ nanoparticles in anatase structure covered GO's nanosheets surface. The electrochemical studies exhibited that TiO₂-GO/CPE had the sensitive, stable and fast response to determine sufentanil, and the limit of detection, sensitivity and the linear range was obtained 0.07nM, 4.1070 μ A/ μ M and 1 to 10 μ M, respectively. Moreover, the study of TiO₂-GO/CPE capability in prepared real samples of urine and human plasma was evidence to acceptable accuracy of performance of TiO₂-GO/CPE for the determination of sufentanil in real samples.

References

1. J.P. Monk, R. Beresford and A. Ward, *Drugs*, 36 (1988) 286.
2. H. Zhang, W. Guan, L. Zhang, X. Guan and S. Wang, *ACS omega*, 5 (2020) 18007.
3. K. Zhang, Z. Yang, X. Mao, X.-L. Chen, H.-H. Li and Y.-Y. Wang, *ACS Applied Materials & Interfaces*, 12 (2020) 55316.
4. K. Zhang, Q. Huo, Y.-Y. Zhou, H.-H. Wang, G.-P. Li, Y.-W. Wang and Y.-Y. Wang, *ACS Applied Materials & Interfaces*, 11 (2019) 17368.
5. K. Yang, Q. Liu, Y. Zheng, H. Yin, S. Zhang and Y. Tang, *Angewandte Chemie*, 133 (2020) 6396.
6. J. Scholz, M. Steinfath and M. Schulz, *Clinical pharmacokinetics*, 31 (1996) 275.
7. Y. Yang, H. Chen, X. Zou, X.-L. Shi, W.-D. Liu, L. Feng, G. Suo, X. Hou, X. Ye and L. Zhang, *ACS Applied Materials & Interfaces*, 12 (2020) 24845.
8. W. Cao, N. Wu, R. Qu, C. Sun, Z. Huo, J.S. Ajarem, A.A. Allam, Z. Wang and F. Zhu, *Environmental Science and Pollution Research*, 28 (2021) 31301.
9. X. Pan, J. Wei, M. Zou, J. Chen, R. Qu and Z. Wang, *Water research*, 194 (2021) 116916.
10. M. Liu, Z. Xue, H. Zhang and Y. Li, *Electrochemistry Communications*, 125 (2021) 106974
11. M. Zou, Y. Qi, R. Qu, G. Al-Basher, X. Pan, Z. Wang, Z. Huo and F. Zhu, *Science of The Total Environment*, 771 (2021) 144743.
12. M. Zhang, L. Zhang, S. Tian, X. Zhang, J. Guo, X. Guan and P. Xu, *Chemosphere*, 253 (2020) 126638.

13. M. Saraji, M.K. Boroujeni and A.A.H. Bidgoli, *Analytical and bioanalytical chemistry*, 400 (2011) 2149.
14. N.F.J. Van Nimmen, K.L.C. Poels and H.A.F. Veulemans, *Journal of Chromatography B*, 804 (2004) 375.
15. C. Dufresne, P. Favetta, C. Paradis and R. Bouliou, *Clinical chemistry*, 47 (2001) 600.
16. A.R. Fakhari, H. Tabani and S. Nojavan, *Analytical Methods*, 3 (2011) 951.
17. L. Liang, S. Wan, J. Xiao, J. Zhang and M. Gu, *Journal of pharmaceutical and biomedical analysis*, 54 (2011) 838.
18. J. Li, F. Wang and Y. He, *Sustainability*, 12 (2020) 10537.
19. L. Zhang, J. Zheng, S. Tian, H. Zhang, X. Guan, S. Zhu, X. Zhang, Y. Bai, P. Xu and J. Zhang, *Journal of Environmental Sciences*, 91 (2020) 212.
20. N. Zhao, L. Deng, D. Luo and P. Zhang, *Applied Surface Science*, 526 (2020) 146696.
21. Z. Savari, S. Soltanian, A. Noorbakhsh, A. Salimi, M. Najafi and P. Servati, *Sensors and Actuators B: Chemical*, 176 (2013) 335.
22. R. Savari, S. Soltanian, A. Noorbakhsh and A. Salimi, *9th Iranian Annual Seminar of Electrochemistry*, 9 (2013) 1.
23. R. Savari, H. Savaloni, S. Abbasi and F. Placido, *Sensors and Actuators B: Chemical*, 266 (2018) 620.
24. Q. Pan, Y. Zheng, Z. Tong, L. Shi and Y. Tang, *Angewandte Chemie International Edition*, (2021)
25. H. Ahmar, A.R. Fakhari, H. Tabani and A. Shahsavani, *Electrochimica Acta*, 96 (2013) 117.
26. Z. Dai, J. Xie, W. Liu, X. Wang, L. Zhang, Z. Zhou, J. Li and X. Ren, *ACS Applied Materials & Interfaces*, 12 (2020) 30289.
27. H. Karimi-Maleh, Y. Orooji, A. Ayati, S. Qanbari, B. Tanhaei, F. Karimi, M. Alizadeh, J. Rouhi, L. Fu and M. Sillanpää, *Journal of Molecular Liquids*, 329 (2021) 115062.
28. K.M. AlAqad, R. Suleiman, O.C.S. Al Hamouz and T.A. Saleh, *Journal of Molecular Liquids*, 252 (2018) 75.
29. R. Mohd Firdaus, N. Berrada, A. Desforges, A.R. Mohamed and B. Vigolo, *Chemistry—An Asian Journal*, 15 (2020) 2902.
30. P.N.O. Gillespie and N. Martsinovich, *ACS Applied Materials & Interfaces*, 11 (2019) 31909.
31. K.D.V. Nguyen and K.D.N. Vo, *AIMS Materials Science*, 7 (2020) 288.
32. H. Karimi-Maleh, M. Alizadeh, Y. Orooji, F. Karimi, M. Baghayeri, J. Rouhi, S. Tajik, H. Beitollahi, S. Agarwal and V.K. Gupta, *Industrial & Engineering Chemistry Research*, 60 (2021) 816.
33. L. Shen, L. Zhang, K. Wang, L. Miao, Q. Lan, K. Jiang, H. Lu, M. Li, Y. Li and B. Shen, *RSC advances*, 8 (2018) 17209.
34. Z. Dai, J. Xie, X. Fan, X. Ding, W. Liu, S. Zhou and X. Ren, *Chemical Engineering Journal*, 397 (2020) 125520.
35. H. Karimi-Maleh, S. Ranjbari, B. Tanhaei, A. Ayati, Y. Orooji, M. Alizadeh, F. Karimi, S. Salmanpour, J. Rouhi and M. Sillanpää, *Environmental Research*, 195 (2021) 110809.
36. H. Zhang, X. Wang, N. Li, J. Xia, Q. Meng, J. Ding and J. Lu, *RSC Advances*, 8 (2018) 34241.
37. C. Rath, P. Mohanty, A. Pandey and N. Mishra, *Journal of Physics D: Applied Physics*, 42 (2009) 205101.
38. R. Hassanzadeh, A. Siabi-Garjan, H. Savaloni and R. Savari, *Materials Research Express*, 6 (2019) 106429.
39. H. Savaloni and R. Savari, *Materials Chemistry and Physics*, 214 (2018) 402.
40. D.S.R. Josephine, K.J. Babu and K. Sethuraman, *Microchimica Acta*, 184 (2017) 781.
41. D. Liao, G. Wu and B. Liao, *Colloids and Surfaces A: Physicochemical and Engineering Aspects*, 348 (2009) 270.
42. P.V. Kumar, M. Bernardi and J.C. Grossman, *ACS nano*, 7 (2013) 1638.

43. H. Tian, C. Wan, X. Xue, X. Hu and X. Wang, *Catalysts*, 7 (2017) 156.
44. H. Karimi-Maleh, M.L. Yola, N. Atar, Y. Orooji, F. Karimi, P.S. Kumar, J. Rouhi and M. Baghayeri, *Journal of colloid and interface science*, 592 (2021) 174.
45. A.T. Smith, A.M. LaChance, S. Zeng, B. Liu and L. Sun, *Nano Materials Science*, 1 (2019) 31.
46. Y. Zhang, N. Zhang, Z.-R. Tang and Y.-J. Xu, *Physical Chemistry Chemical Physics*, 14 (2012) 9167.
47. F. Chahshouri, H. Savaloni, E. Khani and R. Savari, *Journal of Micromechanics and Microengineering*, 30 (2020) 075001.
48. H. Savaloni, E. Khani, R. Savari, F. Chahshouri and F. Placido, *Applied Physics A*, 127 (2021) 1.
49. H. Karimi-Maleh, Y. Orooji, F. Karimi, M. Alizadeh, M. Baghayeri, J. Rouhi, S. Tajik, H. Beitollahi, S. Agarwal and V.K. Gupta, *Biosensors and Bioelectronics*, 184 (2021) 113252.
50. L. Palleschi, L. Lucentini, E. Ferretti, F. Anastasi, M. Amoroso and G. Draisci, *Journal of pharmaceutical and biomedical analysis*, 32 (2003) 329.

© 2021 The Authors. Published by ESG (www.electrochemsci.org). This article is an open access article distributed under the terms and conditions of the Creative Commons Attribution license (<http://creativecommons.org/licenses/by/4.0/>).